Eur Phys J C **40**, s03, 1–8 (2005)
Digital Object Identifier (DOI) 10.1140/epjcd/s2005-03-001-1

EPJ C direct
electronic only

Young Scientist

MSSM Higgs bosons at a future linear collider. Heavy quark production at HERA

T. Klimkovich

DESY, Notkestraße 85, 22607 Hamburg, Germany, e-mail: tklimk@mail.desy.de

Received: 21 January 2005 / Accepted: 28 January 2005 /
Published online: 24 February 2005 –

Abstract. We study the potential of the future e^+e^- linear collider operated at a center-of-mass energy of 500 to 1000 GeV for the measurement of the neutral Higgs boson properties within the framework of the MSSM. The process of associated Higgs boson production with subsequent decays of Higgs bosons into b-quarks is considered. An integrated luminosity of 500 fb^{-1} is assumed at each energy. The Higgs boson masses and production cross sections are measured by reconstructing the $\mathrm{b\bar{b}b\bar{b}}$ final state. The precision of these measurements, depending on the Higgs boson masses, is evaluated. Under the assumed experimental conditions, a statistical accuracy ranging from 0.1 to 1.0 GeV is achievable on the Higgs boson mass. The topological cross section $\sigma(\mathrm{e^+e^-} \to \mathrm{HA} \to \mathrm{b\bar{b}b\bar{b}})$ can be determined with the relative precision of 1.5–6.6 %. The 5σ discovery limit corresponds to the Higgs mass of around 385 GeV for the degenerate Higgs boson masses in the $\mathrm{HA} \to \mathrm{b\bar{b}b\bar{b}}$ channel at $\sqrt{s} = 800$ GeV with integrated luminosity of 500 fb^{-1}. The potential of the Higgs mass determination for the benchmark point SPS 1a for the process $\mathrm{HA} \to \mathrm{b\bar{b}b\bar{b}}$ at $\sqrt{s} = 1$ TeV and luminosity 1000 fb^{-1} is investigated. The possibility of parameter measurements in a CP-violating MSSM scenario is shown. In the second part the inclusive method of charm and beauty cross section measurements in e^+p collisions at H1 experiment for values of $\mathrm{Q}^2 > 12$ GeV^2 is explained. Preliminary plots are shown.

1 MSSM Higgs bosons at a future linear collider

1.1 Introduction

A future e^+e^- linear collider operating at a center-of-mass energy of 500 to 1000 GeV can become an excellent tool for investigating the mechanism of electroweak symmetry breaking. In the minimal Standard Model (SM), breaking of electroweak symmetry is provided by one Higgs doublet, which introduces an additional spin-0 particle, the Higgs boson [1]. A distinct feature of the supersymmetric models is the extended Higgs sector. In the CP-conserving MSSM (Minimal Supersymmetric extension of the Standard Model) the Higgs sector consists of five physical states: two CP-even Higgs bosons, the lighter of which is denoted as h and heavier H, one CP-odd Higgs Boson A and two charged bosons $\mathrm{H}^{\pm}$. The mass eigenstates in this scenario are equal to CP eigenstates. The Higgs sector can be parametrized by $\mathrm{m_A}$ and $\tan\beta$, where $\tan\beta$ is the ratio of the vacuum expectation values of the two Higgs doublets.

In the MSSM it is possible to explicitly or spontaneously break CP symmetry by radiative corrections [2, 3]. The SM fails to provide enough CP-violation to explain the cosmological matter-antimatter asymmetry. CP-violating effects in MSSM can help to reduce this crisis [4]. CP-violation is introduced in the MSSM Higgs potential via loop effects and manifests itself in complex phases of $\mathcal{L}_{\mathrm{MSSM}}$; in particular, the phases of $A_{t,b}$, the soft SUSY-breaking trilinear couplings of the top (bottom) squark to the Higgs boson, and $\mathrm{m_{\tilde{g}}}$, the mass of the gluino. The phase of $A_{t,b}$ is the only parameter to introduce the CP-violation in the Higgs potential on one-loop level. On two-loop level the phase of $\mathrm{m_{\tilde{g}}}$ enters as an additional paramet er, which can provide CP-violation. If CP is broken in the Higgs sector, then the Higgs boson mass eigenstates no longer correspond to CP eigenstates. There are three neutral Higgs bosons $\mathrm{H_1}$, $\mathrm{H_2}$, $\mathrm{H_3}$ ($\mathrm{m_{H_1}} \leq \mathrm{m_{H_2}} \leq \mathrm{m_{H_3}}$) that have mixed CP parities. The parametrization of the Higgs sector is chosen to be in $\mathrm{m_{H^+}}$ and $\tan\beta$, because the Higgs boson A is no longer a mass eigenstate.

The present analysis is motivated by the existing LHC "wedge" region for MSSM Higgs boson production (Fig. 1). There is a large part of the parameter space where ATLAS will be able to see only h^0. A future linear collider can check the MSSM Higgs boson production in that region. In this paper, the study of Higgs boson pair production at a future linear e^+e^- collider is presented. This analysis is an extension of previous studies [6,7]. The analyzed topology is the $\mathrm{b\bar{b}b\bar{b}}$ final state. In the follow-

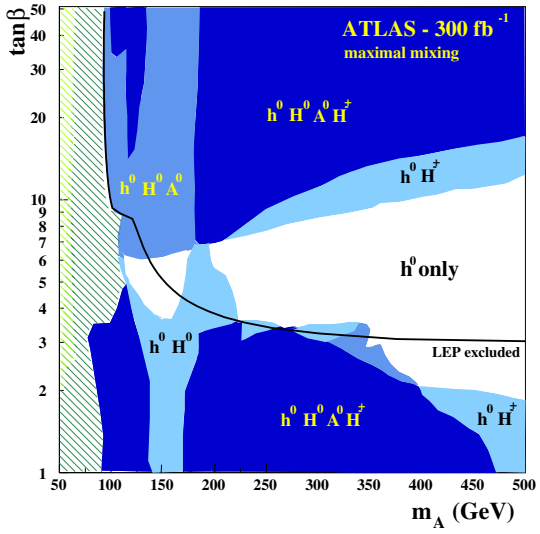

Fig. 1. ATLAS Higgs boson production possibility as a function of parameters m_A and $\tan\beta$

ing we will assume the $e^+e^- \to HA$ production process. However, this assumption does not restrict the generality of our study and the analysis developed in this paper is applicable to the process $e^+e^- \to hA$ as well as to the processes of associated Higgs pair production in CP-violating MSSM scenarios.

The study of the Higgs pair production process is motivated by a so-called 'decoupling limit' of the MSSM, in which the h boson approaches the properties of the SM Higgs boson. The closer the MSSM scenario moves towards the decoupling limit the more difficult it becomes to distinguish the Higgs sector from the SM. In such a scenario the detection of heavier neutral Higgs bosons would be crucial for establishing an extended Higgs sector. The decoupling limit is approached relatively fast for large values of the H and A boson masses, $m_A, m_H >$ 200 GeV, in a large portion of the MSSM parameter space. The most distinct feature of this scenario is the vanishing coupling of heavy CP-even Higgs boson to weak bosons, $\cos(\beta-\alpha) \to 0$:

$$g_{HZZ,HWW} \sim \cos(\beta-\alpha). \quad (1)$$

As a consequence, the H boson production via the fusion and Higgs-strahlung processes is significantly suppressed, whereas the cross section of the $e^+e^- \to HA$ process reaches its maximal value, making associated heavy Higgs pair production a promising channel for the detection of the H and A bosons at a future linear e^+e^- collider:

$$g_{HAZ} \sim \sin(\beta-\alpha). \quad (2)$$

It should also be emphasized that in the decoupling limit the H and A bosons are almost degenerate in mass and have similar decay properties.

1.2 Detector simulations and Monte Carlo samples

The study presented here [5] was performed for a linear collider operating at center-of-mass energies of 500 GeV to 1000 GeV and an event sample corresponding to an integrated luminosity of 500 fb^{-1}.

The detector used in the simulation followed the proposal for the TESLA collider as presented in the TDR [6]. Studies have also been performed in Asia and North America [8,9]. The detector response was simulated with the parametric fast simulation program SIMDET [10]. Beamstrahlung was accounted for using CIRCE [11].

Samples of $e^+e^- \to HA$ events were generated for several Higgs boson mass hypotheses with PYTHIA 6.2 [12], including initial state radiation. The tree level cross section of the HA production was related to the Higgs-strahlung cross section in the SM, σ^{SM}_{HZ}, in the following way [13]:

$$\sigma_{HA} = g^2_{HAZ}\bar{\lambda}_{HA}\sigma^{SM}_{HZ}, \quad (3)$$

where

$$\bar{\lambda}_{HA} = \frac{\lambda^{3/2}_{HA}}{\lambda^{1/2}_{HZ}[12m^2_Z/s + \lambda_{HZ}]} \quad (4)$$

accounts for the suppression of the P-wave cross section near the kinematic threshold. The quantity $\lambda_{ij} = [1 - (m_i + m_j)^2/s][1 - (m_i - m_j)^2/s]$ is the usual momentum factor of the two particle phase space. The Higgs-strahlung cross section in the SM was computed using the program HPROD [14].

For the case of maximal allowed g_{HAZ} coupling, $\sin^2(\beta-\alpha) = 1$, which was assumed for these studies, signal cross sections are given in Table 1. The branching fractions of the Higgs bosons into b-quarks were set to their typical values in the MSSM: $Br(H \to b\bar{b}) = Br(A \to b\bar{b}) = 90\%$. For the background estimation, the following processes were generated using PYTHIA 6.2: $e^+e^- \to WW$, $e^+e^- \to ZZ$, $e^+e^- \to q\bar{q}$. The cross sections for the most important background processes are given in Table 2.

1.3 Analysis tools

Identification of b-quarks plays a crucial role in this analysis. The efficient tagging of jets containing heavy flavour hadrons will be achieved with a highly granular micro-vertex detector, which allows for the precise reconstruction of track parameters in the vicinity of the primary interaction point.

The procedure of tagging b-jets exploits both single track and secondary vertex information. Secondary vertices are searched for within jets using the package ZVTOP [15] developed for the SLD experiment. A neural network is developed [16] for jet flavour separation. The analysis uses a jet-wise tag, referred to hereafter as the jet b-tag variable. It is defined as follows for a jet with neural network output x:

$$B(x) = \frac{f_b(x)}{f_b(x) + f_{udsc}(x)}, \quad (5)$$

where $f_b(x)$ and $f_{udsc}(x)$ are probability density functions of neural network output in samples of b– and udsc–jets, respectively. Tagging of c-jets proceeds in a similar way.

The mass resolution of the reconstructed Higgs bosons is improved by means of a kinematic fit. In the $b\bar{b}b\bar{b}$ analysis, conservation of four-momentum is required, leading to a total of four constraints. The kinematic fit is performed using the code developed by DELPHI [17].

1.4 Analysis procedure and results

Events of the $b\bar{b}b\bar{b}$ topology are characterized by four high multiplicity hadronic jets, which contain the decay products of b-hadrons. A cut-based technique is employed to separate signal from background. Selection criteria are optimized separately for 500 GeV and 800 GeV center-of-mass energies. Each event is required to pass the following cuts:

Table 1. Tree level cross sections σ_{HA} for $e^+e^- \to HA$ expected for the Higgs boson mass hypotheses (m_H,m_A) considered in the study. Numbers are given for $\sin^2(\beta-\alpha)$=1. Cross sections were calculated including ISR at center-of-mass energies of $\sqrt{s}$ = 500, 800 GeV

$\sqrt{s}$ [GeV]	(m_H,m_A) [GeV]	σ_{HA} [fb]
	(150,100)	33.62
	(200,100)	25.30
	(250,100)	16.61
500	(150,140)	28.39
	(150,150)	26.90
	(200,150)	18.85
	(250,150)	10.67
	(200,200)	11.35
	(300,150)	10.55
	(290,200)	9.54
	(300,250)	7.49
800	(300,300)	5.70
	(350,350)	2.23
	(400,150)	6.46
	(400,200)	5.17
	(400,250)	3.70

Table 2. Topological cross sections $\sigma \times BR$ of background processes at $\sqrt{s}$ = 500, 800 GeV

Process	$\sigma \times BR$ [fb]	
	500 GeV	800 GeV
$t\bar{t} \to W^+bW^-\bar{b}$	$6.69 \cdot 10^2$	$1.65 \cdot 10^2$
$WW \to q\bar{q}q\bar{q}$	$4.13 \cdot 10^3$	$2.34 \cdot 10^3$
$ZZ \to q\bar{q}q\bar{q}$	$3.11 \cdot 10^2$	$1.74 \cdot 10^2$
$q\bar{q}(q = u, d, s, c, b)$	$1.29 \cdot 10^4$	$5.45 \cdot 10^3$

1. Total energy deposited in the detector, the visible energy E_{vis}, must be greater than 340 GeV (600 GeV) for 500 GeV (800 GeV) center-of-mass energies.
2. Each event is forced into four jets using the DURHAM algorithm [18] and the number of tracks per jet is required to be greater than three.
3. To separate centrally produced H and A bosons from the WW and ZZ events, peaking in forward/backward direction, we apply a cut on the polar angle of the thrust vector [12], $|\cos\theta_T| < 0.8$.
4. Further suppression of the WW and ZZ backgrounds is achieved by requiring the event thrust value to be less than 0.88.
5. Two-fermion background is suppressed by applying a cut on the DURHAM jet resolution parameter, for which the event changes from four to three jets, $\log_{10} y_{34} \geq -2.9$.
6. High multiplicity six-jet events originating from $e^+e^- \to t\bar{t}$ production are reduced by requiring the number of particle flow objects[1] in the event to be less than 130. This cut is applied only at $\sqrt{s} = 500$ GeV.
7. The background from $e^+e^- \to t\bar{t}$ events is further reduced by applying a cut on the jet resolution parameter, for which the event changes from six to five jets, $\log_{10} y_{56} \leq$ -3.1 (-2.8) at $\sqrt{s} = 500$ GeV (800 GeV).
8. Finally, we make use of the b-tag information to enhance the purity of the selected event sample. First, the b-tag variable for each jet is calculated as described in Sect. 1.3. The four b-tag variables are sorted in descending order, $B_1 > B_2 > B_3 > B_4$. Two quantities B_{12}, B_{34} are then defined as

$$B_{12} = \frac{B_1 B_2}{B_1 B_2 + (1-B_1)(1-B_2)},$$

$$B_{34} = \frac{B_3 B_4}{B_3 B_4 + (1-B_3)(1-B_4)}.$$

The value of B_{12} must be greater than 0.75 (0.6) at $\sqrt{s} = 500$ GeV (800 GeV). The value of B_{34} must be greater than 0.05 independent of the center-of-mass energy.

Events accepted in the final sample are subjected to a 4C kinematic fit. For each of the three possible di-jet pairings, the di-jet mass sum and the di-jet mass difference are reconstructed. In the final step of the analysis, the spectra of the di-jet mass sum and difference, obtained in the $HA \to b\bar{b}b\bar{b}$ channel are used to determine Higgs boson properties.

First, the analysis is performed assuming that the natural widths of Higgs bosons are small relative to detector resolution. As an example Fig. 2 shows the distributions of the di-jet mass sum and di-jet mass difference obtained after selection cuts and kinematic fit in the

[1] The event reconstruction is done in terms of particle flow objects. First, tracks are measured with tracking system and associated to calorimetric clusters to define charged particle flow objects (electrons, muons and charged hadrons). Calorimetric clusters with no associated tracks are regarded as neutral particle flow objects (photons and neutral hadrons).

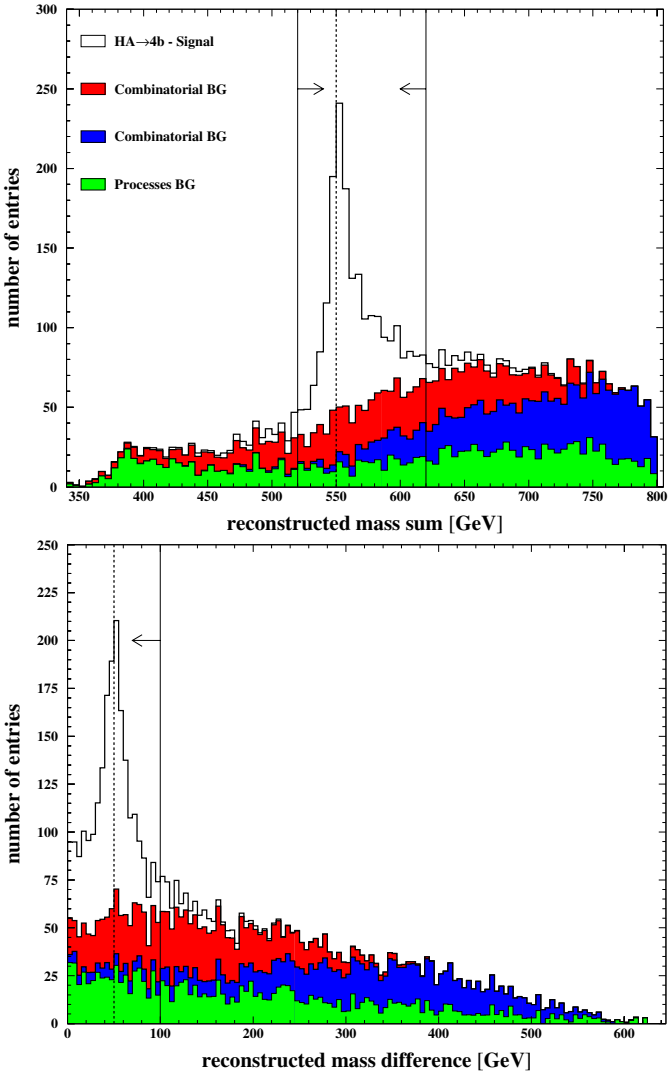

Fig. 2. Distributions of the di-jet mass sum (upper figure) and di-jet mass difference (lower figure) in the HA $\rightarrow$ b$\bar{\text{b}}$b$\bar{\text{b}}$ channel for Higgs boson mass hypothesis (m_{H},m_{A}) = (300,250) GeV at $\sqrt{s}$ = 800 GeV after selection cuts and kinematic fit

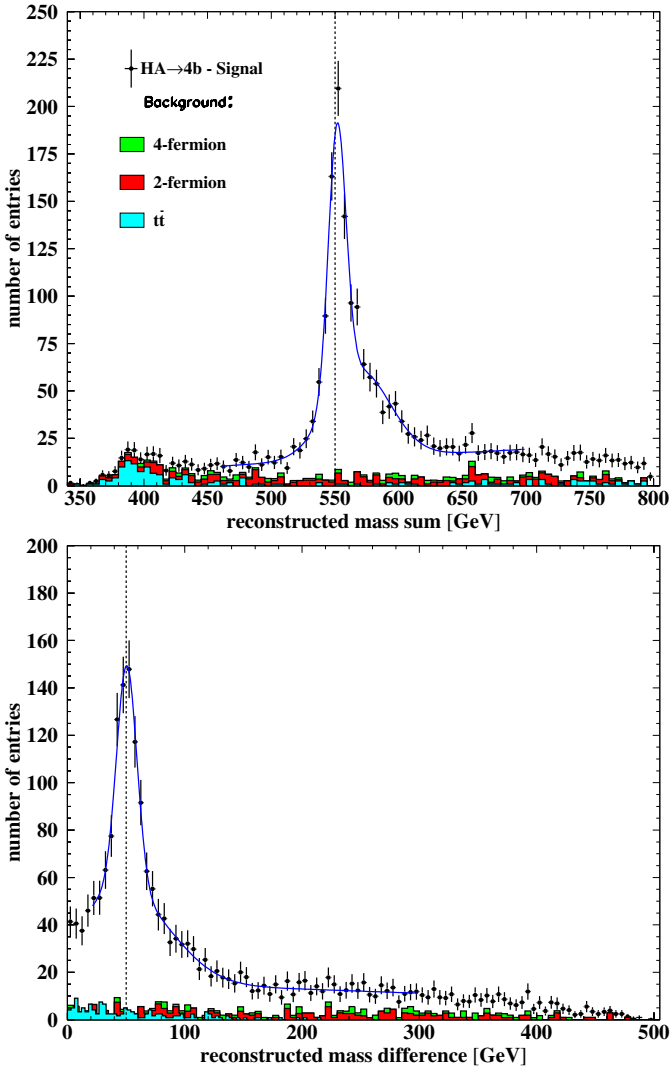

Fig. 3. Upper figure: distribution of the di-jet mass sum after selection cuts, kinematic fit and cut on di-jet mass difference. Lower figure: distribution of the di-jet mass difference after selection cuts, kinematic fit and cut on di-jet mass sum

HA $\rightarrow$ b$\bar{\text{b}}$b$\bar{\text{b}}$ channel for the Higgs boson mass hypothesis of (m_{H},m_{A}) = (300,250) GeV at $\sqrt{s}$ = 800 GeV. Three entries per event contribute to these distributions, corresponding to three possible pairings of jets in the four-jet events. Two entries form a so-called combinatorial background. Figure 3 demonstrates the final di-jet mass sum and di-jet mass difference after the cut on the di-jet mass difference sum, respectively, as indicated by arrows in Fig. 2. Higgs boson masses can be measured with an accuracy ranging from 0.1 to 1 GeV for Higgs pair production above and close to the kinematic threshold. The topological cross section $\sigma(\text{e}^+\text{e}^- \rightarrow \text{HA} \rightarrow \text{b}\bar{\text{b}}\text{b}\bar{\text{b}})$ can be measured with a relative precision varying between 1.5 and 6.6%.

A large part of the SUSY parameter space leads to degenerate H and A Higgs boson masses. For this case the discovery significance as a function of m_H (=m_A) (Fig. 4) is calculated for the HA $\rightarrow$ b$\bar{\text{b}}$b$\bar{\text{b}}$ channel at $\sqrt{s}$ = 800 GeV. Approaching the kinematic limit, the significance drops below 5σ between 380 to 390 GeV. The whole range of the significances for the Higgs masses is from 28.2 to 3.4. Figure 4 also shows η^2 as a function of m_H (=m_A), where η^2 is the assumed $\text{e}^+\text{e}^- \rightarrow$ HA cross section relative to that for $\sin^2(\beta - \alpha) = 1$.

1.5 SPS 1a

The present analysis was applied to one of the so-called benchmark points SPS 1a for SUSY searches [19]. SPS 1 is a typical mSUGRA scenario, which consists of a point with an intermediate value of $\tan\beta$ and a model line attached to it (SPS 1a) and of a "typical" mSUGRA point with relatively high $\tan\beta$ (SPS 1b). The parameters for the SPS 1a point are m_0 = 100 GeV, $\text{m}_{1/2}$ = 250 GeV, A_0 = -100 GeV, $\tan\beta$ = 10, $\mu > 0$. For this point the Higgs

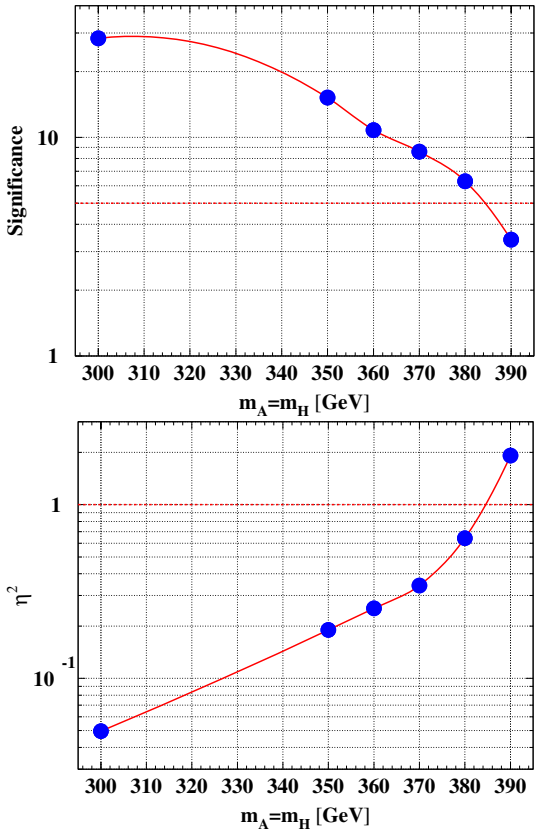

Fig. 4. Discovery significance as a function of the Higgs boson mass (assuming $m_H = m_A$) in the HA $\to$ b$\bar{\text{b}}$b$\bar{\text{b}}$ channel at $\sqrt{s}$ = 800 GeV (upper figure). η^2 as a function of the Higgs boson mass for the 5σ discovery limit (lower figure)

masses are m_{h^0} = 113.7 GeV, m_{A^0} = 394.65 GeV, m_{H^0} = 394.9 GeV, $m_{H^\pm}$ = 403.6 GeV according to the Hdecay and Feynhiggsfast programs [20,21].

The analysis is carried out for the center-of-mass energy of $\sqrt{s}$ = 1 TeV, at which the cross section for the process $e^+e^- \to$ HA is 2.5 fb. The luminosity assumed is 1000 fb^{-1}. The branching ratio for the H (A) Higgs boson to b$\bar{\text{b}}$ is 0.64 (0.40), Γ_{tot} = 0.785 GeV (1.251 GeV).

Figure 5 presents results for the mass sum and the mass difference after selection cuts, kinematic fit and final cuts for the mass difference and the mass sum, respectively. The masses can be measured with precision of 1.3 GeV. The signal efficiency is 29% after selection cuts and 24% after cuts on di-jet mass sum and difference. The cross section can be measured with the relative uncertainty of 9%.

1.6 Measurement of parameters of CP-violating MSSM

CP violation in the MSSM Higgs sector is predominantly mediated by the CP-odd phase of the soft SUSY-breaking trilinear coupling of the Higgs boson to the top and bottom squarks arg($A_{t,b}$) at the one-loop level, with arg($m_{\tilde{g}}$)

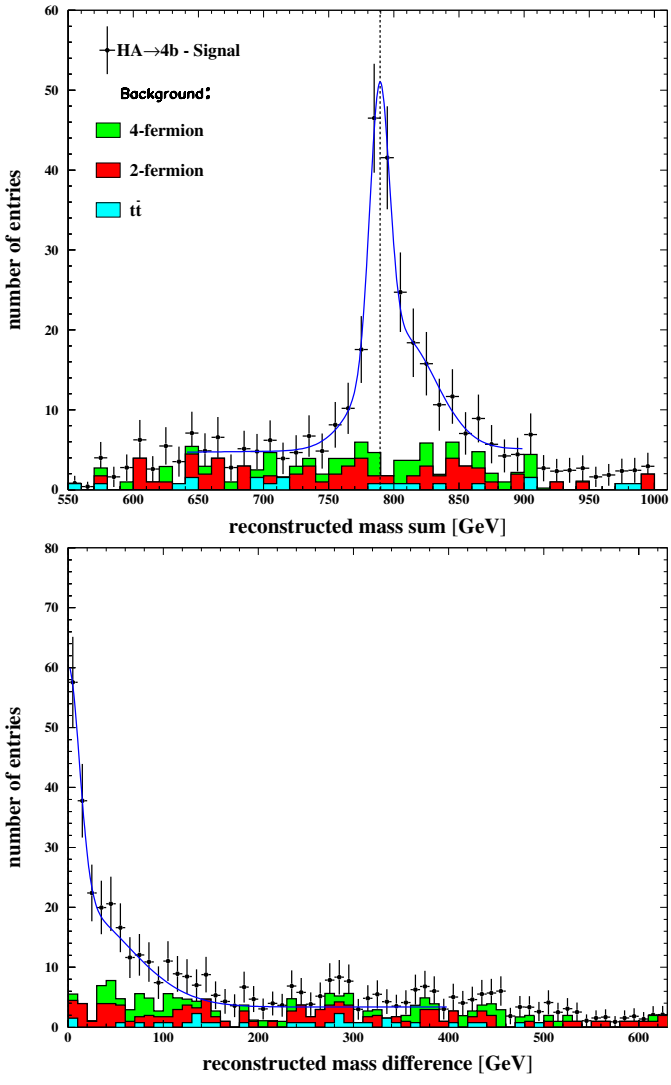

Fig. 5. Upper figure: distribution of the di-jet mass sum after selection cuts, kinematic fit and cut on di-jet mass difference. Lower figure: distribution of the di-jet mass difference after selection cuts, kinematic fit and cut on di-jet mass sum. Both distributions are in the HA $\to$ b$\bar{\text{b}}$b$\bar{\text{b}}$ channel for the SPS 1a benchmark point with Higgs boson mass hypothesis (m_{H},m_{A}) = (394.90,394.65) GeV at $\sqrt{s}$ = 1 TeV

entering at the two-loop level. The CP-violating benchmark scenario is defined as follows [22]:
$\widetilde{M}_Q = \widetilde{M_t} = \widetilde{M_b} = M_{SUSY}$, $\mu = 4M_{SUSY}$,
$|A_t| = |A_b| = 2M_{SUSY}$, $\arg(A_t) = 90°$,
$|m_{\tilde{g}}| = 1$TeV, $\arg(m_{\tilde{g}}) = 90°$.
Assuming the realization of the CP-violating scenario of MSSM, we maintain in the present analysis that tan β and μ could be measured in the chargino sector while m_{H^+} could be measured directly. The remaining free parameters are Im($A_{t,b}$) and Re($A_{t,b}$). We choose tan β = 3 and m_{H^+} = 200 GeV, μ = 2000. For this parameter set it is possible to generate model points in the plane (Im($A_{t,b}$), Re($A_{t,b}$)) an d presuppose that any point chosen is in fact realized in nature. In this case the chosen point has the parame-

Table 3. Parameter values for the chosen point $(\mathrm{Im}(A_{t,b}), \mathrm{Re}(A_{t,b}))$

Parameter	Value
m_{H_1}	95 GeV
m_{H_2}	180 GeV
m_{H_3}	200 GeV
$\tan\beta$	3
m_{H^+}	200 GeV
N_{events}	360

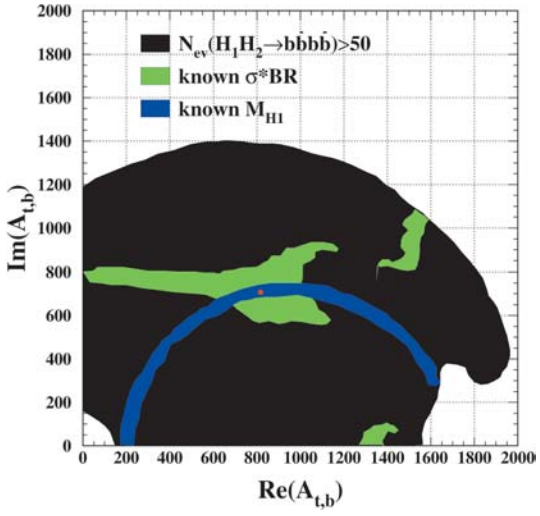

Fig. 6. 1σ deviation for $\sigma \times \mathrm{BR}$ for the process $e^+e^- \to H_1H_2 \to b\bar{b}b\bar{b}$ and m_{H_1} in the case of two variables $\mathrm{Im}(A_{t,b})$ and $\mathrm{Re}(A_{t,b})$

ters presented in Table 3. The analysis was done for the process $e^+e^- \to H_1H_2 \to b\bar{b}b\bar{b}$, with $\sqrt{s} = 500$ GeV, integrated luminosity of 500 fb^{-1} and for the condition that the number of events exceeds 50. The 1σ deviations for the values $\sigma \times \mathrm{BR}$ and m_{H_1} in $\mathrm{Im}(A_{t,b}), \mathrm{Re}(A_{t,b})$ parameter space are presented in Fig. 6. The precision of TESLA measurements for m_{H_1} and m_{H_2} is assumed to be 1 GeV, for $\sigma \times \mathrm{BR}$ it is 10% ([6] or see 1.4). The 1σ region for the combination of $\sigma \times \mathrm{BR}$ and m_{H_1} and m_{H_2} is presented in Fig. 7. As one can see, it is possible to measure $\arg(A_{t,b})$ for this case. The result of the measurement is $\mathrm{Im}(A_{t,b}) = 700 \pm 50$ and $\mathrm{Re}(A_{t,b}) = 800 \pm 300$. The measurement of m_{H_2} in addition to m_{H_1} does not give any new information about the region of the interest.

2 Heavy quark production at HERA using the H1 detector

One of the most important processes to study in quantum chromodynamics (QCD) is heavy quark production. Measurements of the open charm (c) and beauty (b) cross sections in low Q^2 Deep Inelastic Scattering (DIS) at HERA have mainly been done using exclusive methods that are

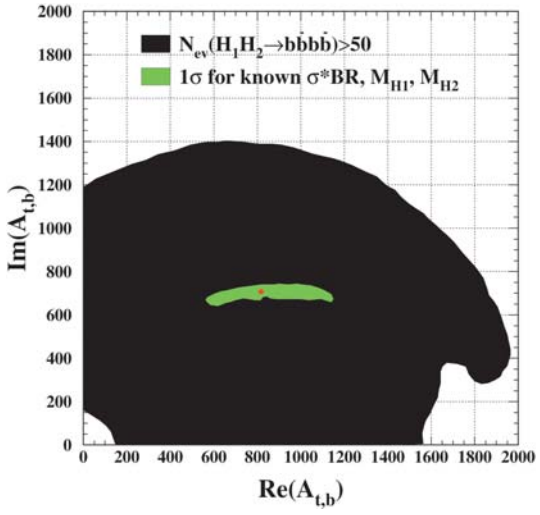

Fig. 7. 1σ region for the combination of $\sigma \times \mathrm{BR}$ for the process $e^+e^- \to H_1H_2 \to b\bar{b}b\bar{b}$, m_{H_1} and m_{H_2} in the case of two variables $\mathrm{Im}(A_{t,b})$ and $\mathrm{Re}(A_{t,b})$

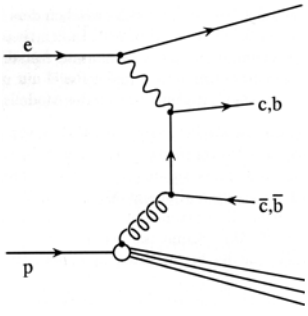

Fig. 8. The process of boson gluon fusion

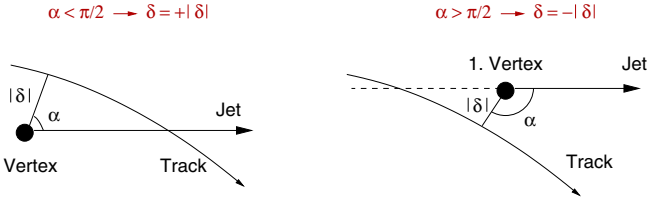

Fig. 9. The DCA is defined as positive if the angle between the jet axis and the line joining the vertex to the point of DCA is less than 90°; otherwise, it is defined as negative

statistically limited [23]. The present analysis is of inclusive c and b cross sections in e^+p scattering at HERA in the range $Q^2 > 12$ GeV^2. Events containing hea vy quarks can be distinguished from light quark events by the long lifetimes of c and b hadrons, which lead to displacements of tracks from the primary vertex. The distance of a track to the primary vertex is reconstructed using precise spatial information from the H1 vertex detector. A similar analysis has already been performed for high Q^2 DIS events [24].

At values of $Q^2 \sim M^2$ the production of heavy quarks is described by the 'massive' scheme [25], in which the heavy

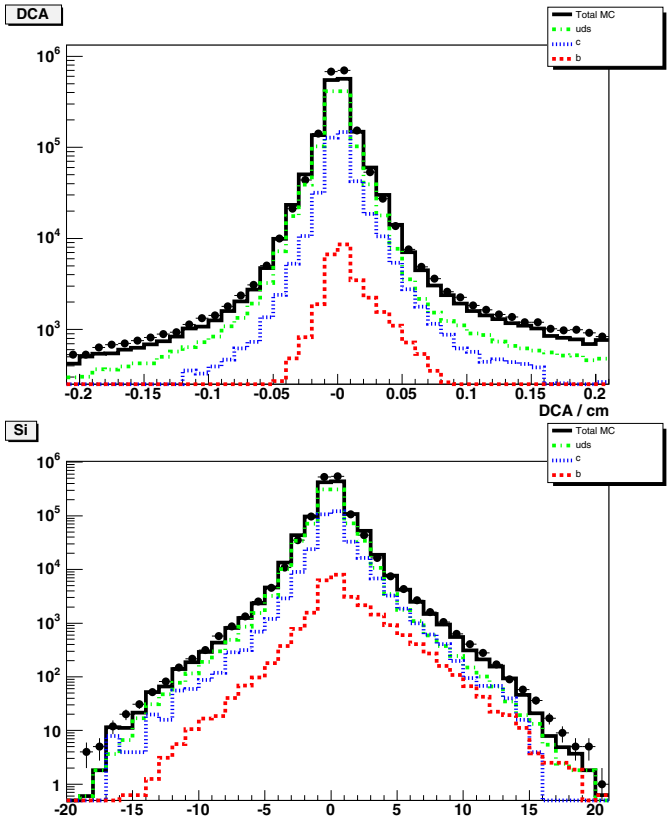

Fig. 10. The distance of closest approach of a track to the vertex (DCA) in the $x-y$ plane (upper plot) and the significance (lower plot) for all CST tracks. Included in the figure is the RAPGAP Monte Carlo [26] after adjusting the contributions from the various quark flavours to the data

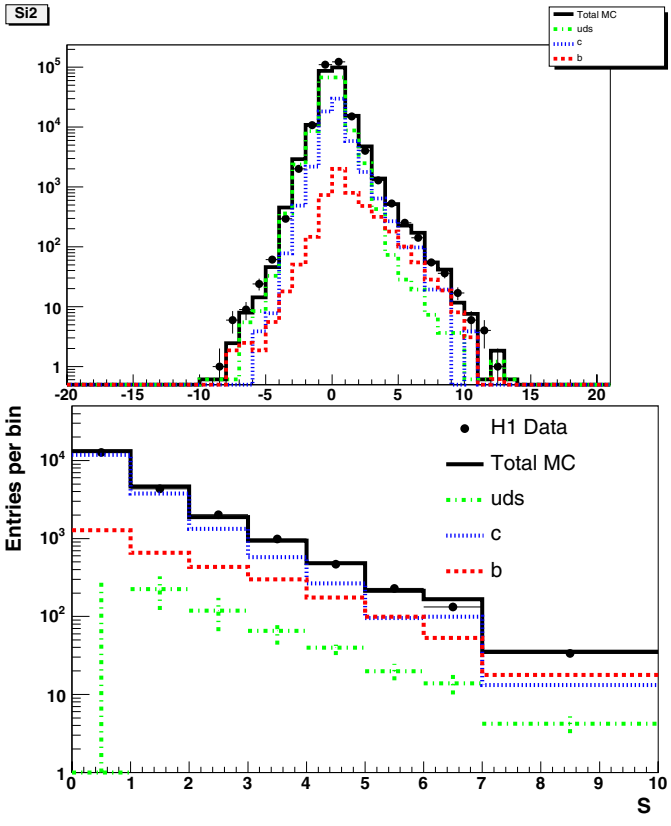

Fig. 11. The significance S_2 distribution per event (upper plot) of the track with the second highest absolute significance for events with ≥ 2 reconstructed CST tracks matched to the jet. The distribution S_2 (lower plot) after subtracting the bins with equal magnitude but negative sign from the positive ones

flavour partons are treated as massive quarks. The heavy quarks are produced perturbatively with their mass providing the hard scale. The dominant leading order (LO) process is boson gluon fusion (BGF) (Fig. 8). The scheme is often referred to as the fixed flavour number scheme (FFNS).

The analysis is based on the low Q^2 data of neutral current (NC) events, collected in the years 1999-2000, when HERA was operated in unpolarised e^+p mode, with an ep centre of mass energy $\sqrt{s} = 318$ GeV. The Monte Carlo program RAPGAP [26] is used to generate low Q^2 NC DIS events for the processes ep $\rightarrow$ eb$\bar{\text{b}}$X, ep $\rightarrow$ ec$\bar{\text{c}}$X, and an inclusive sample is generated using the DJANGO [27] Monte Carlo program. The samples o f events generated for the c and b and inclusive processes are passed through a detailed simulation of the detector response based on the GEANT3 program [28], and through the same reconstruction software as is used for the data.

Charged particles are measured in the central tracking detector (CTD). The CTD tracks are linked to hits in the vertex detector (central silicon tracker CST) to provide precise spatial track reconstruction. In this paper, the CST-improved CTD tracks are called 'CST tracks'. The different quark flavours are distinguished on the basis of the different lifetimes of the produced hadrons. Due to the relatively low cross sections and limited CST track reconstruction efficiency, the decay length of the heavy hadrons is not reconstructed directly. Instead, the transverse distance of closest approach (DCA) of the track to the primary vertex point is used (Fig. 9). Tracks from the decays of long lived particles will mainly have a positive true DCA, but thos e produced at the primary vertex will have zero true DCA. Reconstructed tracks with negative DCA values result mainly from detector resolution.

The DCA distribution of CST tracks associated to the jet axis is presented in Fig. 10. The data appear asymmetric, with positive values exceeding negative values, thus indicating the presence of long lived particles. The data is reasonably well described by the simulation. The light-quark component of the simulation is almost symmetric at low |DCA|. The asymmetry at DCA$\geq$0.1 cm is mostly attributable to long-lived strange particles, such as K_s. The significance, def ined as the ratio of the DCA to its error, is used for better separation of the quark flavours (Fig. 10).

Furthermore, the second significance distribution S_2 (Fig. 11) is defined for events with two or more tracks associated with the jet, and represents the significance of the track with the second highest absolute significance. The

track with the second highest significance is chosen because heavy quarks with more than two tracks are usually produced with high significance, whereas it is highly improbable for light quarks to produce two tracks with large significance due to resolu tion effects. Therefore S_2 gives a better separation power of light from heavy quarks.

For the reduction of the uncertainty due to DCA resolution and light quark normalisation, the negative bins in the S_2 distributions are subtracted from the positive ones. The subtracted S_2 is shown in Fig. 11. As one can see, the resulting distribution is dominated by c quark events, with an increasing b fraction with increasing significance. The contribution of the light quarks is a small fraction for all values of significance.

In the final step, the fractions of c, b and light quarks of the data will be extracted for several $x - Q^2$ intervals by a simultaneous least squares fit to the subtracted S_2 distributions and the total number of inclusive events before track selection, using the Monte Carlo samples as templates.

References

1. P.W. Higgs, Phys. Lett. **12**, 132 (1964); Phys. Rev. Lett. **13**, 508 (1964); Phys. Rev. **145**, 1156; (1966); F. Englert, R. Brout, Phys. Rev. Lett. **13**, 321 (1964); G.S. Guralnik, C.R. Hagen, T.W.B. Kibble, Phys. Rev. Lett. **13**, 585 (1964)
2. A. Pilaftsis, C.E.M. Wagner, Nucl. Phys. B **553**, 3 (1999) hep-ph/9902371
3. M. Carena, J.R. Ellis, A. Pilaftsis, C.E.M. Wagner, Nucl. Phys. B **586**, 92 (2000) hep-ph/0003180
4. M. Carena, J.M. Moreno, M. Quiros, M. Seco, C.E.M. Wagner, Nucl. Phys. B **599**, 158 (2001) hep-ph/0011055
5. K. Desch, T. Klimkovich, T. Kuhl, A. Raspereza, Study of Higgs Boson Pair Production at Linear Collider, hep-ph/0406229, LC-PHSM-2004-006, 2004
6. T. Behnke, S. Bertolucci, R.-D. Heuer, R. Settles, TESLA: The Superconducting Electron-Positron Linear Collider with an Integrated X-Ray Laser Laboratory. Technical Design Report, Part IV : A Detector for TESLA, DESY 2001-011 and ECFA 2001-209 (2001)
7. A. Andreazza, C. Troncon, Study of HA Production in e^+e^- Collisions at $\sqrt{s} = 800$ GeV, DESY-123-E, p. 417
8. S. Kiyoura, S. Kanemura, K. Odagiri, Y. Okada, E. Senaha, S. Yamashita, Y. Yasui, arXiv:hep-ph/0301172
9. T. Abe et al., Linear Collider Physics Resource Book for Snowmass 2001, BNL-52627, CLNS 01/1729, FERMILAB-Pub-01/058-E, LBNL-47813, SLAC-R-570, UCRL-ID-143810-DR, LC-REV-2001-074-US
10. SIMDET V4.0, M. Pohl, H.J. Schreiber, SIMDET: a Parametric Monte Carlo for a TESLA Detector, DESY-02-061 LC-DET-2002-005 (2002)
11. CIRCE V6, T. Ohl, Comp. Phys. Comm. **94**, 53 (1996)
12. T. Sjöstrand, L. Lonnblad, S. Mrenna, PYTHIA 6.2: Physics and Manual, hep-ph/0108264
13. J.F. Gunion, H.E. Haber, G. Kane, S. Dawson, The Higgs Hunter's Guide, Addison Wesley, 1990
14. A. Djouadi, HPROD: A Program for SM and MSSM Higgs Boson Production in e^+e^- Collisions, http://w3.lpm.univ-montp2.fr/~djouadi/GDR/programs/hprod.html
15. D. Jackson, Nucl. Instr. and Meth. A **388**, 247 (1997)
16. S. Xella-Hansen, D.J. Jackson, R. Hawkings, C.J.S. Damerell, Flavour Tagging Studies for the TESLA Linear Collider, LC-PHSM-2001-024
17. N. Kjaer, R. Moller, Reconstruction of invariant masses in multi-jet events, DELPHI Note 91-17 PHYS 88
18. S. Catani, Yu.L. Dokshitzer, M. Olsson, G. Turnock, B.R. Webber, Phys. Lett. B **269**, 432 (1991)
19. B.C. Allanach, M. Battaglia, G.A. Blair, M. Carena et al., hep-ph/0202233
20. A. Djouadi, J. Kalinowski, M. Spira, Hdecay: a program for Higgs boson decays in the Standard Model and its supersymmetric extension, Comput. Phys. Commun. 108:56-74,1998; hep-ph/9704448
21. S. Heinemeyer, W. Hollik, G. Weiglein, Feynhiggs and Feynhiggsfast: programs for higher order calculations in the neutral CP even Higgs boson sector of the MSSM, LC-TH-2001-065, KA-TP-5-2001, 2001. In 2nd ECFA/DESY Study 1998-2001 2393-2421
22. M. Carena, J. Ellis, A. Pilaftsis, C.E.M. Wagner, CP-Violating MSSM Higgs Bosons in the Light of LEP 2, hep-ph/0009212, 2000
23. F. Sefkow, Heavy Quark Production in Deep-Inelastic Scattering, hep-ex/0110036, 2001
24. Measurement of $F_2^{c\bar{c}}$ and $F_2^{b\bar{b}}$ at high Q^2 using the H1 Vertex Detector at HERA, H1 Preliminary
25. E. Laenen, S. Riemersma, J. Smith, W.L. van Neerven, Nucl. Phys. B **392**, 162 (1993); E. Laenen, S. Riemersma, J. Smith, W.L. van Neerven, Nucl. Phys. B **392**, 229 (1993); S. Riemersma, J. Smith, W.L. van Neerven, Phys. Lett. B **347**, 143 (1995) hep-ph/9411431
26. H. Jung, Comput. Phys. Commun. **86**, 147 (1995) (see also http://www.desy.de/ jung/rapgap/)
27. H. Charchula, G.A. Schuler, H. Spiesberger, Comput. Phys. Commun., **81**, 381 (1994) (see also http://www.desy.de/ hspiesb/django6.html)
28. R. Brun, R. Hagelberg, M. Hansroul, J.C. Lassalle, CERN-DD-78-2-REV